IMAGE BASED MULTISCALE MODELING OF POROUS BIOMATERIALS

JUDY P. YANG[1*], J. S. CHEN[2], SHENG-WEI CHI[3]

[1]*Assistant Professor, Department of Civil Engineering, National Chiao Tung University, Hsinchu 30010, Taiwan, R.O.C.*

[2]*Professor, Department of Civil and Environmental Engineering, University of California, Los Angeles (UCLA), Los Angeles, CA 90095, U.S.A.*

[3]*Assistant Professor, Department of Civil and Materials Engineering, University of Illinois at Chicago, Chicago, IL 60607, USA*

ABSTRACT

Biomaterials are typical structures of poroelasticity in nature. Due to heterogeneous composition of microstructures, the asymptotic based homogenization was introduced to correlate the microscopic solid-fluid phase to the macroscopic balance laws. In this work, a microstructure informed computational method for modeling of porous biomaterials is developed. To construct microscopic models directly from medical images, the active contour model based on variational level set formulation for interface and boundary identification is first introduced, which overcomes the difficulties such as the jagged interface, background noise, and blurred objects commonly encountered in the numerical simulation. Inspired by the discretized image pixels, the direct strong form with collocation in conjunction with the reproducing kernel approximation is introduced to solve the level set equation. A gradient reproducing kernel collocation method (Chi et al. 2013) requiring only first order differentiation of approximation functions is then introduced for solving characteristic functions efficiently in the microstructures using pixels as the discretization points. Finally, an image based multiscale modeling of porous biological materials with application to bones is performed to demonstrate the proposed method (Yang et al. 2012).

Keywords: Image based modeling, Gradient reproducing kernel collocation method, Meshfree method, Homogenization, Porous media.

1. INTRODUCTION

For bone materials composed of solid and fluid phases in their microstructures, the poroelasticity such as Biot's theory (Biot 1941) has been introduced to describe bone mechanics (Cowin 1999). Nevertheless, the continuum mixture theory does not provide the explicit relationship between the microstructural composition and the macroscopic characters. Homogenization methods have been

* Corresponding author and presenter: Email: jpyang@nctu.edu.tw

introduced to provide a multiscale paradigm for analysis of poroelastic materials, and yield macroscopic balance laws that resemble Biot's theory while embedding microscopic features (Hollister et al. 1991; Yang et al. 2012). Motivated by the emergence of high resolution digital imaging techniques such as micro-CT and micro-MRI, the investigation of mechanical properties of bones can be estimated more precisely, however, with challenges remaining to be resolved. The jagged interface and sharp corner caused by converting image pixels into finite elements lead to localized responses. Thus, avoiding distorted elements during image reconstruction and mesh generation is a tedious task. The background noise and blurred objects from high-resolution images could lead to incorrect numerical predictions due to geometry errors in the simulation models. A computational framework that can effectively model biological materials at various length scales is of an urgent need for advancement of bioscience. This work introduces an image based strong form collocation method in conjunction with image segmentation for multiscale modeling of bones.

2. LEVEL SET METHOD FOR IMAGE SEGMENTATION

The level set method was originally devised to track the topological changes and has been extensively applied in computer graphics, image processing, and optimization, etc. The spirit of the method utilizes the implicit level set representation in N dimensions to present a surface in $N-1$ dimensions and track its evolution in space effectively. The motion of the level set function controls the boundary evolution. Here we introduce the active contour model (Chan and Vese 1999) for image segmentation and interface identification based on the Mumford-Shah functional with a level set formulation. This technique can detect objects from images with sharp or blurred interfaces.

2.1. Variational Level Set Formulation

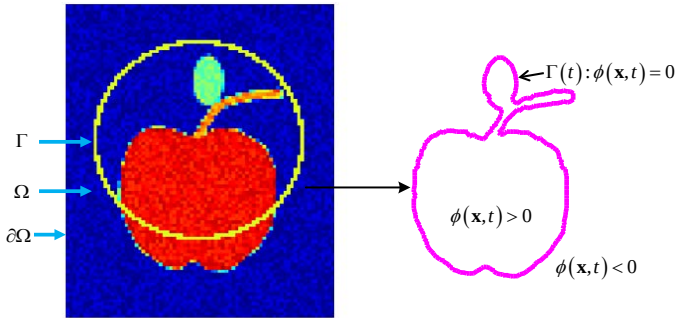

Figure 1: Level set function.

Consider an image enclosed by an open region Ω with the boundary $\partial\Omega$ in R^n and presented by the color code $C(\mathbf{x})$ in Figure 1, a closed evolving interface Γ is placed as the trial interface of the image. The Lipschitz continuous level set function $\phi(\mathbf{x},t)$ is also defined. The image contains two regions, the object to be detected (Ω^i) and the remaining region (Ω^0). Based on the Mumford-Shah functional for image segmentation, define a least-squares functional as follows:

$$\Pi\left(\bar{c}_1,\bar{c}_2,\Gamma\right)=\mu\cdot Length\left(\Gamma\right)+\nu\cdot Area\left(inside\ \Gamma\right)$$
$$+\lambda_1\int_{\text{inside }\Gamma}\left(C\left(\mathbf{x}\right)-\bar{c}_1\right)^2 d\mathbf{x}+\lambda_2\int_{\text{outside }\Gamma}\left(C\left(\mathbf{x}\right)-\bar{c}_2\right)^2 d\mathbf{x} \tag{1}$$

where $\mu\geq 0$, $\nu\geq 0$, $\lambda_1,\lambda_2>0$; $\bar{c}_1$ and $\bar{c}_2$ are the averages of $C(\mathbf{x})$ inside and outside Γ, respectively. For an initial trial Γ^0, the minimization of (1) drives Γ^0 toward the true boundary of the object $\partial\Omega^i$. The first two terms control the smoothness of the detected boundary while the last two measure the errors of the trial interface. With the geometric parameters in terms of $\phi(\mathbf{x},t)$, the stationary of the functional gives the level set equation:

$$\begin{aligned}
&\frac{\partial\phi}{\partial t}=\delta\left(\phi\right)\left[\mu\nabla\cdot\left(\frac{\nabla\phi}{\left|\nabla\phi\right|}\right)-\nu-\lambda_1\left(C\left(\mathbf{x}\right)-\bar{c}_1\right)^2+\lambda_2\left(C\left(\mathbf{x}\right)-\bar{c}_2\right)^2\right] \quad \text{in } \Omega\\
&\phi\left(\mathbf{x},0\right)=\phi_0\left(\mathbf{x}\right) \quad \text{in } \Omega\\
&\delta\left(\phi\right)\frac{\nabla\phi}{\left|\nabla\phi\right|}\cdot\mathbf{n}=0 \quad \text{on } \partial\Omega
\end{aligned} \tag{2}$$

3. HOMOGENIZATION OF POROUS MICROSTRUCTURES

As detailed in (Yang et al. 2012), for a quasi-static poroelastic medium with fluid of low viscosity, through the asymptotic expansion and two-scale decomposition of the two-phase medium, the homogenized macroscopic equilibrium and continuity equations, and generalized Darcy's law are

$$\begin{aligned}
&\int_\Omega \bar{C}_{ijkl}\frac{\partial u_k^0}{\partial x_l}\frac{\partial \varpi_i^0}{\partial x_j}d\Omega-\int_\Omega \bar{\alpha}_{ij}p^0\frac{\partial \varpi_i^0}{\partial x_j}d\Omega=\int_\Omega \bar{f}_i^S\varpi_i^0 d\Omega+\int_{\Gamma_{St}}\bar{t}_i^S\varpi_i^0 d\Gamma\\
&\int_\Omega\frac{\partial}{\partial x_i}\left(\frac{\partial u_i^0\left(\mathbf{x},t\right)}{\partial t}\right)\omega d\Omega+\int_\Omega\frac{\partial}{\partial x_i}\left(\rho^F b_j^F-\frac{\partial p^0\left(\mathbf{x}\right)}{\partial x_j}\right)\bar{K}_{ij}\omega d\Omega=0\\
&\bar{v}_i=\frac{\partial u_i^0\left(\mathbf{x},t\right)}{\partial t}-\bar{K}_{ij}\frac{\partial\bar{P}}{\partial x_j}
\end{aligned} \tag{3}$$

4. IMAGE BASED MICROSCOPIC CELL MODELING

Upon constructing microscopic models directly from images, we introduce the gradient reproducing kernel collocation method (G-RKCM) to solve the level set equation and the characteristic functions defined in the microscopic cell problems (Yang et al. 2012). The gradient RK approximation is introduced for enhanced computational efficiency (Chi et al. 2013).

4.1. Gradient Reproducing Kernel Approximation

The reproducing kernel approximation $\mathbf{u}\left(\mathbf{x}\right)\approx\mathbf{v}\left(\mathbf{x}\right)=\sum_{I=1}^{N_s}\Psi_I\left(\mathbf{x}\right)\mathbf{a}_I$ with N_s source points is considered. The RK shape function is given by

$$\Psi_I(\mathbf{x}) = \mathbf{H}^{\mathrm{T}}(\mathbf{0})\mathbf{M}^{-1}(\mathbf{x})\mathbf{H}(\mathbf{x}-\mathbf{x}_I)\varphi_a(\mathbf{x}-\mathbf{x}_I) \tag{4}$$

where $\varphi_a(\mathbf{x}-\mathbf{x}_I)$ is the kernel function, $\mathbf{H}(\mathbf{x}-\mathbf{x}_I)$ is the monomial basis vector, and the moment matrix is $\mathbf{M}(\mathbf{x}) = \sum_{I=1}^{N_s} \mathbf{H}(\mathbf{x}-\mathbf{x}_I)\mathbf{H}^{\mathrm{T}}(\mathbf{x}-\mathbf{x}_I)\varphi_a(\mathbf{x}-\mathbf{x}_I)$.

For second order differential equations, it is time-consuming to take second order differentiation on the RK shape functions. Thus, we introduce the gradient RK approximation of $\mathbf{u}_{,\beta}$

$$\mathbf{u}_{,\beta} \approx \mathbf{w}_\beta = \sum_{I=1}^{N_s} \Psi_I^\beta(\mathbf{x})\mathbf{a}_I \tag{5}$$

where $\beta = (\beta_1, \beta_2, \ldots, \beta_d)$, $|\beta| = \sum_{i=1}^{d} \beta_i \le k$ for $\Psi_I^\beta \in C^k$. For q th order monomial basis, the gradient RK shape function is given by

$$\Psi_I^\beta(\mathbf{x}) = (-1)^{|\beta|} D^\beta \mathbf{H}^T(\mathbf{0})\mathbf{M}^{-1}(\mathbf{x})\mathbf{H}(\mathbf{x}-\mathbf{x}_I)\varphi_a(\mathbf{x}-\mathbf{x}_I) \tag{6}$$

5. TRABECULAR BONE MODELING

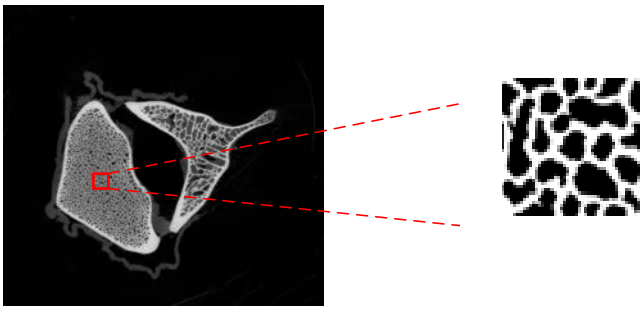

Figure 2: Image of a vertebra with a specified microscopic cell discretized by 45×45 pixels.

In Figure 2, the trabecular bone image of a sheep vertebra adapted from SCANCO Medical is obtained by Xtreme-CT with nominal resolution of 41 μm. A $10mm\times10mm$ microscopic cell specified by a red square is presented by 45×45 pixels. The Young's modulus is $1192\,MPa$, Poisson's ratio is 0.3, and the blood viscosity is $4.373\times10^{-3}\,Pa\cdot s$. The effective Young's moduli, Poisson ratio, the effective stress coefficient tensor, and the homogenized permeability tensor are summarized in Table 1, which agree well with the experimental results (Mittra et al. 2005; Nauman et al. 1999). For the permeability measured in trabecular bones, the reported data in literature has a wide span due to flow direction, bone porosity, and microstructural morphology such as trabecular architecture and separation for various anatomical sites.

Table 1: Homogenized material constants

Material Constants	Numerical Prediction	Experiment
$\bar{E}_{11}\left(MPa\right)$	318.6	$359 \pm 104 \sim 542 \pm 78$
$\bar{E}_{22}\left(MPa\right)$	342.8	
$\bar{\nu}_{12}$	0.1714	–
$\bar{\nu}_{21}$	0.1844	
$\bar{\alpha}_{11}$	0.2571	–
$\bar{\alpha}_{22}$	0.2545	
$\bar{K}_{11}\left(m^2\right)$	2.80×10^{-8}	$10^{-8} \sim 10^{-14}$
$\bar{K}_{22}\left(m^2\right)$	2.27×10^{-8}	

6. CONCLUSIONS

The multiscale homogenization is introduced to correlate the macro- and micro-mechanical behaviors of poroelastic materials, from which the homogenized macroscopic continuity and equilibrium equations, and the generalized Darcy's law were obtained. For an elastic solid with Newtonian fluid of low viscosity, the homogenized macroscopic continuity and equilibrium equations reassemble the governing equations in Biot's theory. To effectively construct microstructures with multi-phases from medical images, we introduced the active contour model for interface and boundary identification without the need of CAD procedures in mesh based methods. Inspired by the pixel points, we introduced the G-RKCM to solve the level set equation and the microscopic cell problems, in which determined linear systems with only first order differentiation are needed. A multiscale modeling of trabecular bone microstructure is presented. The ability to solve the microstructure with complex geometry by the proposed image based framework is demonstrated.

7. ACKNOWLEDGMENTS

This research was conducted possible through the previous study and support at UCLA. The continuing investigation is sponsored by the National Science Council via grant number NSC 101-2218-E-009-010.

REFERENCES

Biot MA (1941). General theory of three-dimensional consolidation. Journal of Applied Physics. 12, pp. 155-164.

Chan T and Vese L (1999). An active contour model without edges. In Lecture Notes in Computer Science 1687, eds. M. Neilsen, P. Johansen, O.F. Olsen and J. Weickert. pp. 141-151.

Chi SW, Chen JS, Hu HY, Yang JP (2013). A Gradient Reproducing Kernel Collocation Method for Boundary Value Problems. International Journal for Numerical Methods in Engineering. 93, pp.1381-1402.

Cowin SC (1999). Bone poroelasticity. Journal of Biomechanics. 32, pp. 217-238.

Hollister SJ, Fyhrie DP, Jepsen KJ, and Goldstein SA (1991). Application of homogenization theory to the study of trabecular bone mechanics. Journal of Biomechanics. 24, pp. 825-839.

Mittra E, Rubin C, and Qin YX (2005). Interrelationship of trabecular mechanical and microstructural properties in sheep trabecular bone. Journal of Biomechanics. 38, pp. 1229-1237.

Nauman EA, Fong KE, Keaveny TM (1999). Dependence of intertrabecular permeability on flow direction and anatomic site. Annals of Biomedical Engineering. 27, pp. 517-524.

SCANCO Medical, http://www.scanco.ch/.

Yang JP, Chi SW, Chen JS (2012). “Image Based Multiscale Modeling of Porous Bone Materials,” Multiscale Simulations and Mechanics of Biological Materials, [Eds. S. Li, D. Qian], Wiley.